NANO LETTERS

2008
Vol. 8, No. 3
767-774

Fullerene Nanocage Capacity for Hydrogen Storage

Olga V. Pupysheva, Amir A. Farajian, and Boris I. Yakobson*

Department of Mechanical Engineering & Materials Science and Department of Chemistry, Rice University, Houston, Texas 77005

Received June 16, 2007; Revised Manuscript Received August 18, 2007

ABSTRACT

We model fullerene nanocages filled with hydrogen, of the general formula $H_n@C_k$, and study the capacity of such endohedral fullerenes to store hydrogen. It is shown using density functional theory that for large numbers of encapsulated hydrogen atoms, some of them become chemisorbed on the inner surface of the cage. A maximum of 58 hydrogen atoms inside a C_{60} cage is found to still remain a metastable structure, and the mechanism of its breaking is studied by ab initio molecular dynamics simulations. Hydrogen pressure inside the fullerene nanocage is estimated for the first time and is shown to reach the values only a few times smaller than the pressure of hydrogen metallization. We provide a general relation between the hydrogen pressure and resulting C−C bond elongation for fullerene nanocages of arbitrary radii. This opens a way to assess possible hydrogen content inside larger carbon nanocages, such as giant fullerenes, where significant capacity can be reached at reasonable conditions.

Among the intriguing properties of carbon nanostructures, the possibility to synthesize endohedral fullerenes or nanotubes containing various atoms and molecules is interesting for various possible applications.[1] In such composites a fullerene or nanotube plays the role of nanocage whose inner cavity is filled with a foreign compound.[2,3] In particular, existence of endohedral fullerenes with a hydrogen molecule inside, predicted theoretically in 1991,[4] makes the idea of storing hydrogen inside a fullerene cage especially attractive. Although the interaction between the hydrogen and the storage media is weaker in this case than for a conventional chemisorption, a high potential barrier of breaking the cage stabilizes the hydrogen inside it. We note that the potential of giant hollow molecules to entrap "hundreds of times their own weight" of some small molecules was considered by Daedalus as early as in 1966.[5]

Endohedral C_{60} fullerene containing one H_2 molecule can be produced with high yield[7] by a so-called "molecular surgery" approach.[6,8] Synthesis under high hydrogen pressure using laser excitation is also demonstrated.[9] Insertion of hydrogen into fluorinated carbon cages is considered as another possibility in refs 10 and 11. For the recent progress in hydrogen storage inside carbon nanotubes, see the reviews in refs 3, 12, and 13 and references therein. The latest idea is an elegant "fill-and-lock" mechanism suggested in ref 14.

The task of producing an endohedral fullerene with a higher hydrogen content, although experimentally challenging, can be approached theoretically. Modeling hydrogen storage in fullerene nanocages should answer three basic questions. First, how is hydrogen put inside the cage? Second, how can the release of hydrogen from the cage be controlled? And third, what are the properties of endohedral fullerenes filled with hydrogen? The present study addresses the latter question using C_{60} fullerene as an example. This problem concerns mainly the following issues: maximum sustainable number of encapsulated hydrogen atoms, formation energy of such endohedral complexes, and pressure produced by hydrogen inside the carbon cage.

There are a few theoretical papers considering endohedral C_{60} fullerene containing more than one hydrogen molecule.[15–24] The results of semiempirical optimizations[15–18,23] (followed by density functional[15,23] or Hartree−Fock[17,18] energy calculations) and force field methods[19,20] appear contradictory. The maximum amount of hydrogen to form a stable $H_n@C_{60}$ composite, was determined as 23,[15,23] 24,[16] or 25[17,18] molecules. It was shown[15,17,18] that putting a larger amount of hydrogen led to breaking of one or few C−C bonds of the carbon cage, although details of this process were not studied. From the other side, Dolgonos[19] and Dodziuk[20,22,24] insisted that there was not enough space for more than one hydrogen molecule inside C_{60}. They supported this statement by the calculated highly positive values of stabilization (formation) energy of the $H_n@C_{60}$ complexes. There is also a disagreement regarding the possibility of hydrogen chemisorption on the inner walls of the fullerene, which was observed in refs 17 and 18, while in the other studies all encapsulated hydrogen was found in the molecular form.[15,16,23]

This shows the necessity to use more accurate methods for the structural optimizations of the $H_n@C_{60}$ composites.

10.1021/nl071436g CCC: $40.75
Published on Web 10/09/2007

In this work we use density functional theory (DFT) and study the formation energy and optimized geometry for various n values. We also perform ab initio molecular dynamics (MD) simulations in order to investigate the stability of the optimized structures.

Furthermore, after investigating the hydrogen pressure inside C_{60}, we find a general relation between the internal pressure and expansion of a fullerene nanocage of an arbitrary radius. This opens a way to make our results transferrable, e.g., to giant fullerenes or nanotubes, that is, to predict the possible hydrogen content inside them without repeating ab initio calculations, which are overly expensive for such large systems.

Method. We study the properties of endohedral C_{60} fullerene containing n hydrogen atoms using DFT. The calculations are carried out by SIESTA code.[25–27] Direct diagonalization of the Kohn−Sham Hamiltonian[28] is employed for the electronic structure calculations. Generalized gradient approximation (GGA) with Perdew−Burke−Ernzerhof (PBE) exchange-correlation functional[29] is used. The core electrons are represented by improved Troullier−Martins norm-conserving pseudopotentials.[30] Sankey finite-range pseudo atomic orbitals (PAOs)[31] are utilized as the split-valence double-ζ basis set with polarization (DZP)[32] for valence electrons. A cutoff energy of 125 Ry is used for the grid integration. Structural optimizations are performed by means of conjugate gradient (CG) method, until the residual force on each atom becomes smaller than 0.01 eV/Å. In some cases, a few different starting atomic configurations are used to find the geometry corresponding to the lowest local energy minimum. The DFT-based MD simulations are done by SIESTA in the canonical regime; i.e., the thermodynamical system under consideration is described by the number of particles N, volume V, and temperature T as variables. The structure under study is in contact with Nosé thermostat having fixed temperature 300 K. The MD time step is 1.0 fs.

The accuracy of our method is tested by comparison of optimized geometries of fullerene C_{60}, hydrogen H_2, and some hydrocarbon molecules (methane, ethylene, benzene, etc.) against the existing experimental data. With the pseudopotentials, bases, and other settings specified above, SIESTA tends to slightly overestimate the bond lengths, while the valence angles are determined with 0.1° accuracy. In particular, the calculated and experimental[33] values of H−H bond length in hydrogen molecule equal 0.775 and 0.741 Å, respectively; the calculated and experimental[34] bond lengths of the single C−C bond of C_{60} molecule (i.e., the bond fusing a pentagon and a hexagon) are 1.460 and 1.458 Å, while for the double bond of the fullerene (fusing two hexagons) these values are 1.410 and 1.401 Å, respectively. These deviations from experiment are small enough to rely on the results of the present study.

Results and Discussion. A. Formation Energy of $H_n@C_{60}$ Structures. We relax the structures of general formula $H_n@C_{60}$, where the number of hydrogen atoms n is even, as we are aiming for a system in singlet spin state.

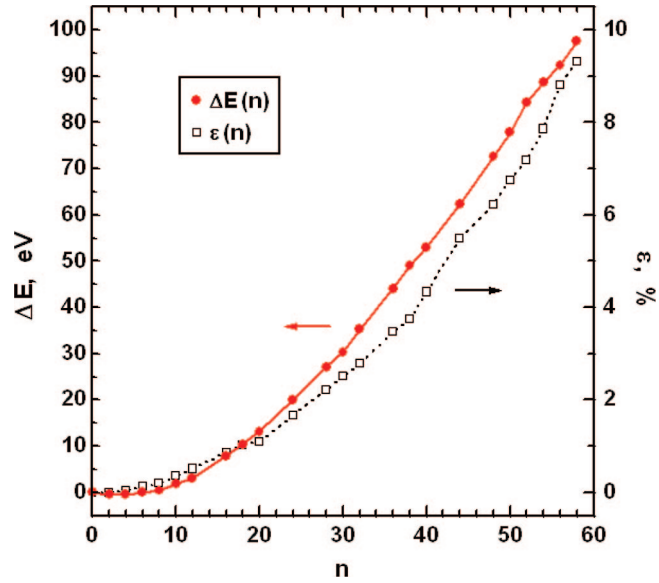

Figure 1. Formation energy (solid line) and average relative C−C bond elongation (dotted line) vs number of encapsulated hydrogen atoms in $H_n@C_{60}$ structures.

Formation energy of the endohedral fullerene containing n hydrogen atoms is defined as

$$\Delta E = E(H_n@C_{60}) - E(C_{60}) - \frac{n}{2}E(H_2)$$

E(X) being the total energy of a free molecule X in its optimized geometry (X = $H_n@C_{60}$, C_{60}, or H_2).

The dependence of the formation energy on n is shown in Figure 1. This curve has a minimum for $n = 2$ (one hydrogen molecule), followed by a monotonous increase, in agreement with the previous studies.[15,16,20,23] The ΔE values are negative for one or two encapsulated H_2 molecules and almost zero for three of them.[35] All the structures with larger n have positive formation energies, i.e., are metastable. We should emphasize that, although some of these structures are highly endothermic and unlikely to form,[19,20,22,24] they still correspond to the local minima of potential energy surfaces, in accord with refs 15–18, 21, and 23.

The last metastable structure in the $H_n@C_{60}$ family contains $n = 58$ encapsulated hydrogens and has a huge formation energy of almost 100 eV (approximately 0.85 eV/atom). No potential energy minima are found for larger numbers of hydrogen atoms. The hydrogen content of $H_{58}@C_{60}$ is approximately 7.5 wt %, which formally exceeds the U.S. Department of Energy (DOE) target for the year 2010 (see, e.g., ref 13).

B. Geometry of $H_n@C_{60}$ Structures. With increase of n, the highly compliant hydrogen densifies significantly, while the nanocage expands slowly (see Figure 2). The average relative elongation of the fullerene C−C bonds is defined as

$$\epsilon(n) = \langle d/d_0 \rangle - 1$$

where d and d_0 are the bond lengths in $H_n@C_{60}$ and ideal C_{60}, respectively. This dependence is shown in Figure 1 by the dotted line and will be used later in this paper.

The average relative C−C bond elongation has a minimum for the first structure in the $H_n@C_{60}$ family ($n = 2$), i.e., simultaneously with the formation energy. This corresponds to a small contraction of all C−C bonds of the nanocage, with a negative value $\epsilon \approx -0.007\%$. Then cage elongation grows monotonously with n, and its maximum of 9.3% for $n = 58$ almost reaches the onset of C−C bond breaking (11%[15] or 14.5%[36]).

Figure 2 shows some typical optimized geometries of $H_n@C_{60}$ for $n = 10$, 30, and 50. The fullerene shape deviates from a sphere for a large amount of encapsulated hydrogen, as is clear from Figure 2c.

For a relatively small number of encapsulated hydrogen atoms, $n < 20$, all the hydrogen inside C_{60} exists only in molecular form, in agreement with refs 15, 16, and 23. The bond length in H_2 molecules varies from 0.75 to 0.80 Å, which is close to one in a free molecule. Hydrogen molecules are organized into clusters of well-defined shapes, such as a tetrahedron for $n = 8$, trigonal bipyramid for $n = 10$, as shown in Figure 2a, and octahedron for $n = 12$, similar to the previous optimization results.[15,23]

For a larger number of encapsulated H atoms, H_2 remains the major form of hydrogen inside the fullerene cage, although not the only one. Namely, for $20 \leq n \leq 40$, a few triangular H_3 molecules are formed, such as in Figure 2b. They exhibit H−H bond lengths in the interval 0.82−1.13 Å, that is, close to or slightly larger than the 0.845 Å equilibrium distance in the lowest stable state of neutral H_3 molecule.[37] Formation of triatomic hydrogen in our structures can be explained by the stabilization of this state by the surrounding polarizable media, i.e., by the encapsulating fullerene.

Importantly, for the structures with $n \geq 30$, some hydrogen atoms form covalent bonds with the carbons of the fullerene cage, as one can see from parts b and c of Figure 2. This differs from some semiempirical results,[15,16,23] but agrees with the statements of Koi and Oku[17,18] and Dodziuk,[20] even though in the latter work hydrogen chemisorption was called "unphysical". Chemical bonding to the inner surface of the fullerene should not be considered as an artifact. It is well-known that chemisorption on the convex surface of nanotubes, and especially fullerenes, is much more favorable than that on their concave surface, as the carbon p-orbital participating in bond formation is mainly localized outside due to the carbon pyramidalization.[38] Nevertheless, the chemisorption on the inner surface of the fullerene is still possible under high pressure.

The length and strength of the carbon−hydrogen bonds depend on the amount of encapsulated hydrogen. For example, the calculated C−H bond lengths are 1.20−1.22 Å in $H_{30}@C_{60}$, 1.15−1.23 Å in $H_{40}@C_{60}$, and 1.10−1.19 Å in $H_{58}@C_{60}$ (cf. 1.11 Å in a free methane molecule). This decrease of the average C−H bond length is due to the higher hydrogen density and pressure in the structures with larger n. Longer C−H distances of 1.26−1.29 Å are also observed for the structures with 48−54 hydrogen atoms, when the chemisorbed H atom is situated close to the nearest H_2 molecule, such that there may be a weak $H\cdots H_2$ interaction in addition to C−H bonding.

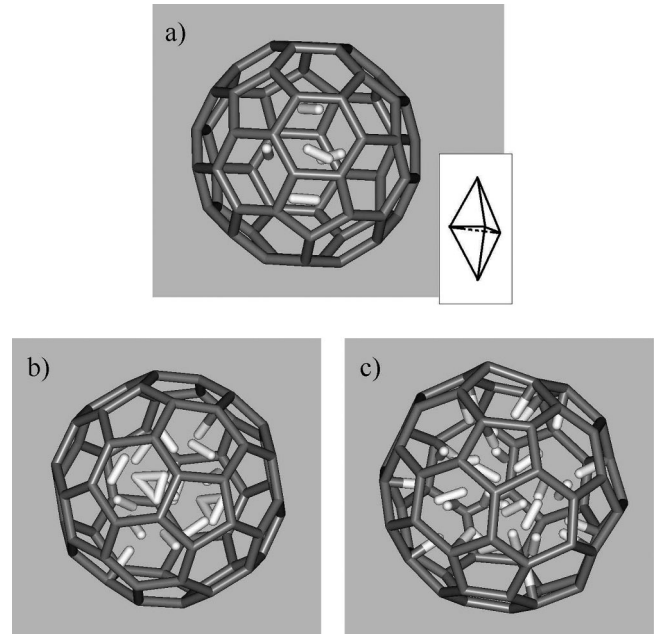

Figure 2. Optimized geometries of $H_n@C_{60}$ structures with (a) $n = 10$ (inset: trigonal bipyramid formed by H_2 molecules), (b) $n = 30$, and (c) $n = 50$. Carbon and hydrogen atoms are shown in gray and white colors, respectively.

The fullerene surface of the $H_n@C_{60}$ structures possessing C−H bonds is deformed, such that the pyramidalization angle of the carbon atom becomes more favorable for chemisorption, i.e., it is closer to the sp^3 hybridization. That is, the surface is flattened in the vicinity of a hydrogenized carbon atom, which is compensated by its larger curvature at the nearest unhydrogenized atoms. This deformation of the carbon cage is especially pronounced in the structures with a large number of C−H bonds, such as the one presented in Figure 2c.

Importantly, the hydrogenized carbon atoms no longer contribute to the conjugated π-system of C_{60}. This breaks the fullerene aromaticity and consequently weakens the cage.

C. Mechanism of Fullerene Nanocage Opening. Different initial geometries of the same general composition $H_n@C_{60}$ often lead to different local energy minima as a result of structural optimizations. For the last structure in this family, $n = 58$, the initial atomic configurations become particularly important. Although we are able to obtain an optimized geometry of $H_{58}@C_{60}$, presented in Figure 3a, relaxation of a different initial structure leads to the breaking of the fullerene nanocage.

The mechanism of cage opening is illustrated by ab initio MD simulations (Figure 3). We start with the optimized structure $H_{58}@C_{60}$, which is put in contact with a thermostat at room temperature. The C−C bonds of the fullerene cage are long, some of them reaching almost 1.70 Å, and thus they are very weak and easy to break. Due to the large amount of hydrogen confined in the fullerene cage, as many as 20 of its carbon atoms are hydrogenized. In addition, three more carbons are situated rather close (within 1.35 Å) to the nearest H_2 molecules, which allows a partial C−H interaction.

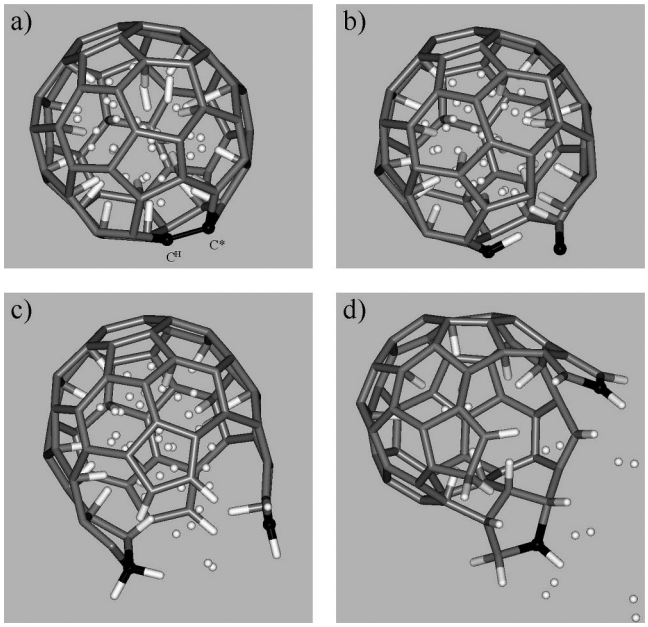

Figure 3. Snapshots of ab initio molecular dynamics simulations of $H_{58}@C_{60}$ structure at 300 K: (a) 0 fs, (b) 250 fs, (c) 350 fs, and (d) 800 fs. Breaking of bond between two carbon atoms shown in black initiates cage opening.

Behavior of two carbon atoms, shown in black in Figure 3a, is especially important for the process of fullerene breaking. One of them, which we will henceforth denote as C^H, is situated close to the nearest hydrogen molecule and partially interacts with one of its atoms (C^H-H distance is 1.30 Å). The other selected carbon atom, C*, is not hydrogenized, but all three of its nearest neighbors form a full or partial C−H bond. As a result, the unhybridized p-orbital of C* partially overlaps only with the corresponding atomic orbital of C^H atom. The length of the C^*-C^H bond is 1.51 Å, while the other two bonds involving the C* atom are yet longer (1.64 and 1.67 Å).

Atomic movements during MD simulations lead to the full hydrogenation of C^H atom. The partial π-bond between C* and C^H breaks and C* becomes a radical, while the remaining C^*-C^H σ-bond is too weak to keep the two atoms together. As one can see from Figure 3b, this bond is already broken after 250 fs. Then the hydrogen bound to C^H quickly changes its position such that this carbon atom restores sp^2 hybridization. Internal pressure pushes hydrogen toward the opened hole in the fullerene surface. This results in the further hydrogenation of C^H (among other carbon atoms), leading to a CH_2-group formation, as shown in Figure 3c. This makes the process of fullerene breaking irreversible. The escape of H_2 molecules from the cage and hydrogenation of the remaining carbons are shown in Figure 3d. We can conclude that the cage opening is promoted by the breaking of one of the weak C−C bonds formed by a carbon atom, all of whose nearest neighbors are fully or partially hydrogenized.

D. Hydrogen Pressure on a C_{60} Nanocage. Estimating the pressure of hydrogen encapsulated in the nanocage meets some difficulties, because its volume at the nanoscale cannot be strictly defined. Furthermore, one fails to find a normal direction to the fullerene surface (and normal components of the atomic forces) when the cage is strongly deformed. In order to find the internal pressure P, we need some well-defined characteristic of the cage, which depends on P. The average relative C−C bond elongation ϵ is chosen for this purpose.

Let us consider a structure obtained by symmetrical expansion of the ideal C_{60}. Relative elongation of all C−C bonds in such structure equals

$$\epsilon = R/R_0 - 1$$

where R and R_0 are the radii of the expanded and relaxed fullerene, respectively.

The force on the kth atom, $\mathbf{F}_k$, is produced by the rest of the carbon atoms and points inside the fullerene. Its normal component equals

$$F_k^{\perp} = (\mathbf{F}_k \cdot \mathbf{R}_k)/R$$

where $\mathbf{R}_k$ is the radius vector from the cage center of mass to the kth atom ($|\mathbf{R}_k| = R$).

The pressure from inside, which compensates these contracting forces, is the sum of $F_k^{\perp}$ for all atoms ($k = 1, ..., 60$) taken with the opposite sign and divided by the cage surface area $A = 4\pi R^2$.

$$P = -\frac{\sum_{k=1}^{60} F_k^{\perp}}{A} = -\frac{\sum_{k=1}^{60} (\mathbf{F}_k \cdot \mathbf{R}_k)}{4\pi R^3} \quad (1)$$

The forces $\mathbf{F}_k$ are computed for expanded structures with various ϵ, and the resulting pressure is plotted in Figure 4a. If there is no chemical interaction between the cage and the encapsulated material, eq 1 is quite general and does not depend on the origin of the internal pressure.

Combination of this $P(\epsilon)$ dependence with $\epsilon(n)$ calculated earlier (see Figure 1) gives us the hydrogen pressure P as a function of the number of encapsulated hydrogen atoms, as depicted in Figure 4b. Notice the negative hydrogen pressure for $n = 2$, which corresponds to the contraction of this endohedral fullerene.

Hydrogen pressure in $H_{58}@C_{60}$ reaches approximately 130 GPa, or 1.3 Mbar. For comparison, a pressure of about 3.5 Mbar is needed for hydrogen metallization.[40] Moreover, the maximum P value calculated here for a fullerene nanocage is of the order of magnitude of the hydrogen pressure in the giant planets Jupiter and Saturn.[40]

E. Internal Pressure on an Arbitrary Fullerene Nanocage. Using our data, it is possible to estimate the internal pressure on a carbon nanocage of an arbitrary size. In order to do so, let us estimate the dependence $P(\epsilon)$ from continuum mechanics and compare it with our results.

Consider a continuous spherical cage of radius R, made of a material with an in-plane stiffness C. A cross section dividing it into two hemispheres has an area $s = \pi R^2$ and circumference $l = 2\pi R$. By definition of the in-plane stiffness, the attracting force between the hemispheres under consideration equals $Cl\epsilon$, where ϵ is the relative elongation of the cage material normal to the cross section. On the other hand, this force is a product of the internal pressure P in the

cage by the cross section s. Then the internal pressure is connected with the relative cage elongation by the following formula

$$P = C\frac{l}{s}\epsilon = \frac{2C\epsilon}{R} \quad (2)$$

where the cage radius itself depends on the elongation, $R = R_0(1 + \epsilon)$.

The function defined by eq 2 is plotted in Figure 4a by the dotted line using the C value for graphite, $C_0 = 360$ N/m.[39] This shell model works remarkably well for the elongations up to 3–4%, and the two $P(\epsilon)$ curves in Figure 4a, calculated using eqs 1 and 2, almost coincide.

For large ϵ, the C−C bonds of the fullerene are too long and far less rigid than those in graphite. Then we can generalize the in-plane stiffness C as

$$C(\epsilon) = \frac{P(\epsilon)R_0(1+\epsilon)}{2\epsilon}$$

with the P values calculated for the C_{60} nanocage using eq 1. This function is depicted in Figure 5a for elongations up to 10%. Notice that the calculated in-plane stiffness is a genuine mechanical property of C_{60} fullerene and does not depend on the nature of the internal pressure, as long as the chemical structure of the fullerene is not changed. Moreover, since the C values are so similar for C_{60} and for graphite, it is reasonable to assume that they are close for the other fullerene cages as well.

This leads to an important generalization, which allows us to predict the relative elongation of any fullerene cage under given pressure, and vice versa. The internal pressure needed to produce a given ϵ depends only on the radius R_0 of the undeformed cage, as shown by the set of hyperbolas in Figure 5b. The vertical lines in Figure 5b mark the radii of some typical nearly spherical fullerenes.[41]

F. Hydrogen Content in Arbitrary Fullerene Nanocage. To find roughly the amount of encapsulated hydrogen $n(\epsilon)$ producing a given relative elongation ϵ in any near-spherical fullerene cage, one needs to estimate the cage inner volume. Also, this requires a knowledge of the equation of state relating the hydrogen density with pressure at the temperature of interest, together with the $P(R_0,\epsilon)$ dependence discussed above.

For a cage of an average radius R, let us define the volume V of a polyhedron with vertices at the centers of the carbon atoms, as well as at the centers of mass of the fullerene pentagons and hexagons. This volume is smaller than the volume of the sphere of radius R but still scales as R^3 with a very good accuracy.

The volume V_{in} occupied by hydrogen inside the fullerene cage is smaller than V, as there is a layer in the vicinity of the cage which cannot be accessed by the hydrogen atoms (see Figure 7). We estimate the thickness δ of this layer based on the $H_n@C_{60}$ optimized geometries obtained earlier. Only the systems without chemisorption are considered, i.e., $n < 30$ and $\epsilon < 2.5\%$ (which correspond to the internal pressures below 50 GPa). The minimum C−H distance prior to a covalent bond formation equals 1.8 Å (achieved for the highest hydrogen content in this interval, $n = 28$). It is impossible to define what part of this distance belongs to which atom; however, knowing that van der Waals radii of hydrogen and carbon are in the ratio 1:1.5, and their covalent radii are in the ratio 1:2, we can roughly assume that in our system the radii of H and C atoms are also in the ratio 1:2. Then the thickness of the unaccessible to hydrogen layer inside the nanocage is $\delta = 1.2$ Å.

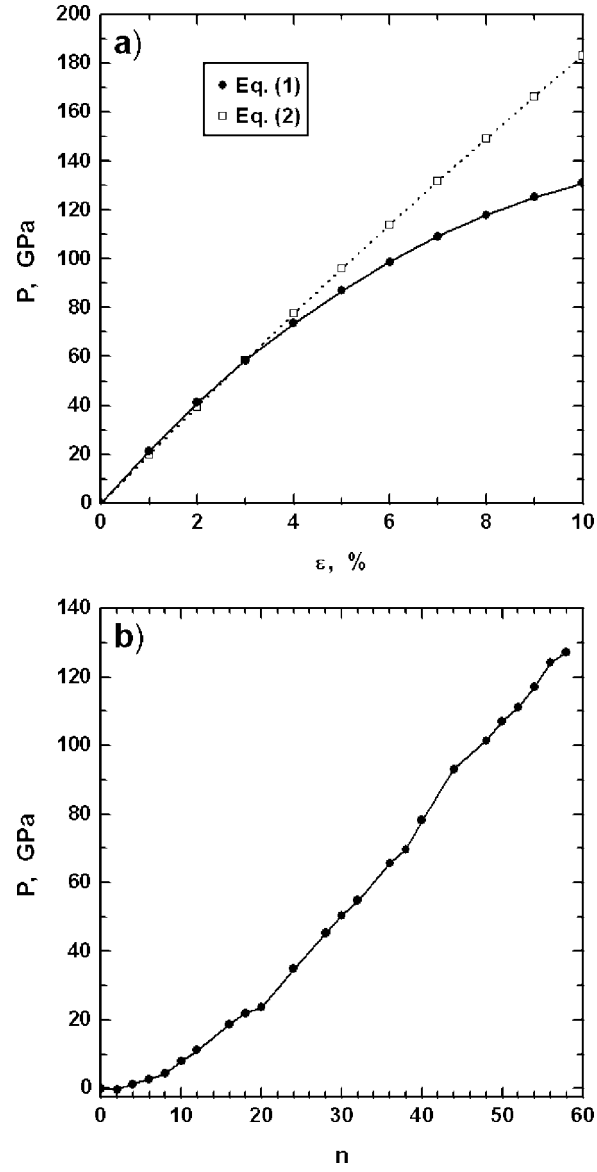

Figure 4. (a) Internal pressure in empty C_{60} fullerene vs produced relative C−C bond elongation, calculated by eq 1 (solid line) and eq 2 (dotted line). (b) Hydrogen pressure on carbon cage vs number of encapsulated hydrogen atoms in $H_n@C_{60}$ structures.

The inner volume of a fullerene nanocage of radius R, which is occupied by hydrogen, is determined by the radius $R - \delta$

$$V_{in}(\epsilon) \approx V_{00}\left[\frac{R-\delta}{R_{00}}\right]^3 = V_{00}\left[\frac{R_0(1+\epsilon)-\delta}{R_{00}}\right]^3 \quad (3)$$

R_{00} and V_{00} being the R and V values for C_{60} in undeformed state (or for any other fullerene chosen as a reference).

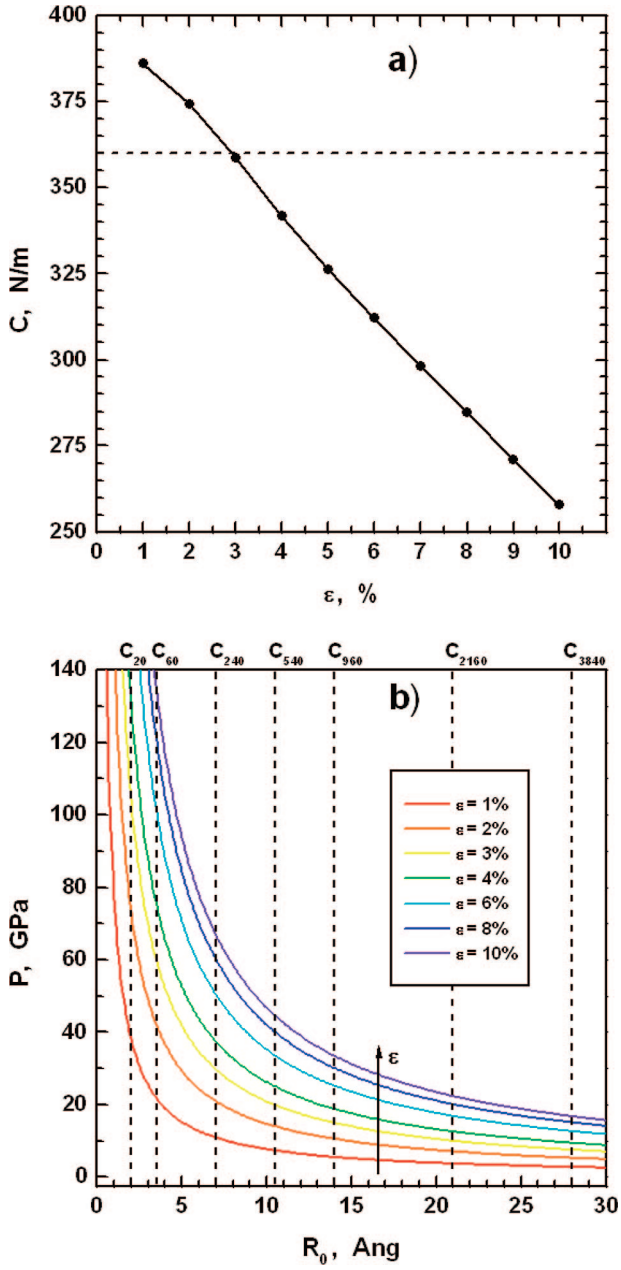

Figure 5. (a) In-plane stiffness of C_{60} fullerene vs C−C bond elongation. Horizontal dashed line marks in-plane stiffness of graphite. (b) Internal pressure in fullerene nanocage producing various average relative C—C bond elongations (ϵ = 1%, 2%, 3%, 4%, 6%, 8%, and 10%) vs radius of undeformed cage. Vertical dashed lines mark radii of some nearly spherical fullerenes.

Knowing $\epsilon(n)$ for the C_{60} cage, we obtain an estimate of the density of encapsulated hydrogen

$$\rho(n) = \frac{nM}{N_A V_{in}(\epsilon(n))} \tag{4}$$

where M = 1 g/mol is the molar mass of hydrogen atom and $N_A = 6.02 \times 10^{23}$ mol^{-1} is the Avogadro number.

Combining the functions $\varrho(n)$ and $P(n)$ obtained earlier, we plot the hydrogen density versus pressure (see Figure 6a). The noticeable increase of density at $P \approx 22$ GPa corresponds to the appearance of triatomic hydrogen mol

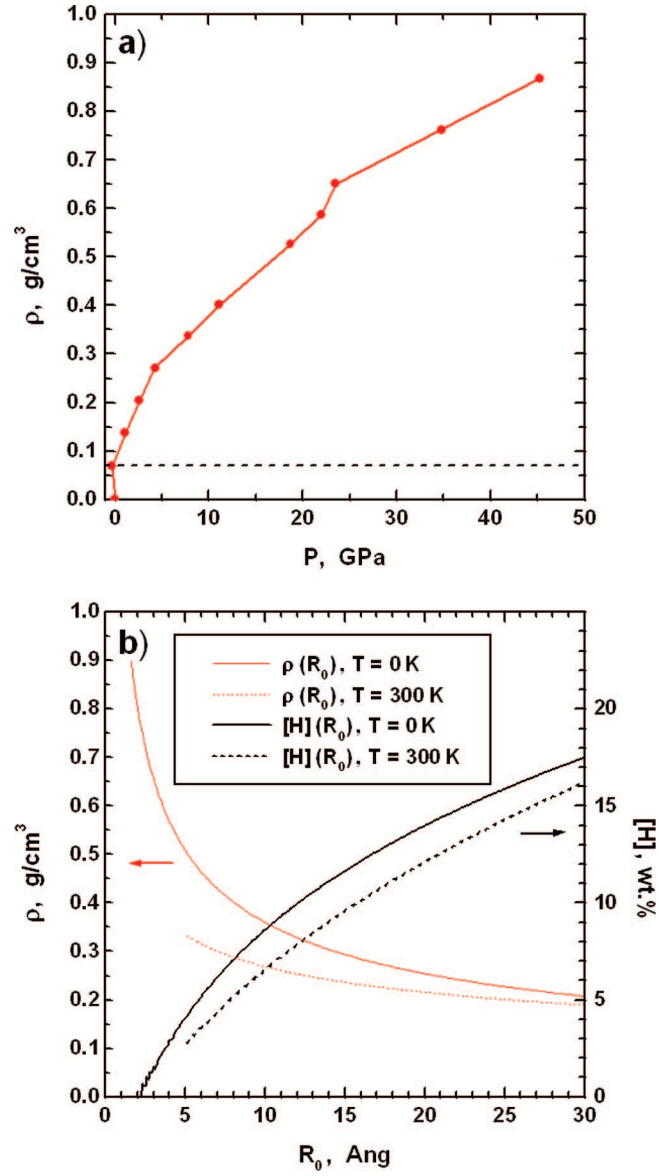

Figure 6. (a) Estimated hydrogen density in $H_n@C_{60}$ structures vs hydrogen pressure. Horizontal dashed line marks the density of liquid hydrogen at boiling point (20 K) under ambient pressure. (b) Estimated hydrogen density in $H_n@C_{60}$ structures with 1% average relative C−C bond elongation (thin lines) and corresponding hydrogen content (thick lines) vs radius of undeformed cage, based on eqs 3 and 4 for T = 0 K (solid lines), and eqs 5 and 6 for T = 300 K (dashed lines).

ecules in addition to H_2, which is observed for $H_n@C_{60}$ structures with $n \geq 20$.

Next, we compare these calculated hydrogen densities at zero temperature with $\rho(P)$ values for room temperature, e.g., using the available experimental data of ref . Putting T = 300 K in the equation of state,[42] we obtain the H_2 molar volume

$$V_{mol}(P) = a_1 P^{-1/3} + a_2 P^{-2/3} + a_3 P^{-1} \tag{5}$$

with the empirical coefficients a_1 = 16.2 GPa$^{1/3}$ cm^3/mol, a_2 = –4.3 GPa$^{2/3}$ cm^3/mol, and a_3 = 2.6 GPa cm^3/mol, valid for pressures below 15 GPa. Correspondingly, the hydrogen density at 300 K equals

$$\rho = \frac{2M}{V_{\mathrm{mol}}} \qquad (6)$$

where the factor 2 corresponds to two hydrogen atoms in a H_2 molecule, and M, as before, is the hydrogen atomic mass per mole.

Using eqs 3 and 4 or eqs 5 and 6 for zero or room temperature, respectively, we can find the hydrogen density inside any nearly spherical fullerene nanocage C_k, producing the relative average C−C bond elongation ϵ. These functions $\rho(R_0)$ are plotted in Figure 6b for the parameter value $\epsilon = 1\%$. Recall that they are meaningful in the interval $P < 50$ GPa (that is, $R_0 > 1.5$ Å) for $T = 0$ K, and $P \leq 15$ GPa ($R_0 \geq 5.1$ Å) for $T = 300$ K.

Product of hydrogen density ϱ and volume V_{in} gives us the mass of encapsulated hydrogen. The parabolic dependence of the number of carbon atoms k on the corresponding fullerene radius $R_0(C_k)$ allows us to estimate the mass of carbon and, thus, the hydrogen gravimetric content[H]. Figure 6b depicts the[H] values at rather safe 1% average strain of the fullerene nanocage, as functions of radius R_0, for zero and room temperatures.

For example, let us consider a typical giant fullerene such as C_{720} (for recent discussion see ref 43). Its radius is $R_0 = 12.7$ Å, and a pressure of about 6 GPa is necessary to get the C−C bond elongation of 1% (see Figure 5b). Then the inner volume of the cage equals $V_{\mathrm{in}} = 5.7 \times 10^{-21}$ cm^3, while the hydrogen density ρ is estimated to be 0.32 and 0.25 g/cm^3 for zero and room temperature, respectively (see Figure 6a). Consequently, to expand C_{720} fullerene only by 1%, it should be filled with more than 1000 hydrogen atoms at zero temperature, or with more than 800 atoms at 300 K. A cross section of the latter structure, optimized using semiempirical potentials, is schematically shown in Figure 7. The n values estimated here correspond to the hydrogen content over 10 wt % or over 8 wt % for $T = 0$ or 300 K, respectively. This by far exceeds the DOE target of 6.0 wt %.[13]

The numbers presented here demonstrate the excellent mechanical properties of the fullerene cages, which can keep a large amount of a foreign compound in their inner cavity without being significantly deformed.

Conclusions. We study the properties of $H_n@C_{60}$ structures using density functional theory. Their formation energy, average relative elongation of the fullerene C−C bonds, and hydrogen pressure inside the fullerene nanocage are calculated as functions of the number of hydrogen atoms n. Although structures with a large amount of encapsulated hydrogen are highly endothermic, they still correspond to the local minima of the potential energy surface. It is found that for large n, some hydrogen atoms can be chemisorbed on the inner surface of the carbon cage; i.e., they can form covalent C−H bonds. The maximum number of hydrogen atoms inside C_{60}, which can form a metastable structure, i.e., corresponds to an energy minimum, is determined to be $n = 58$. The mechanism of $H_{58}@C_{60}$ breaking is studied by ab initio molecular dynamics simulations at room temperature. It is shown that the hydrogen chemisorption, which weakens the fullerene C−C bonds, plays the key role in the opening of the nanocage.

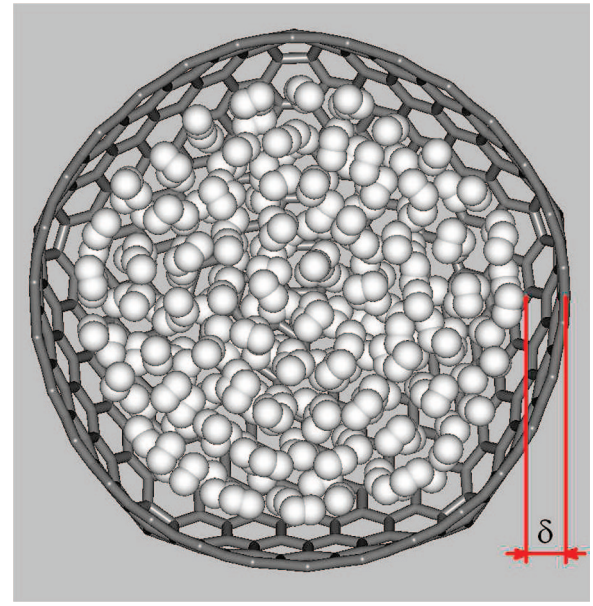

Figure 7. Cross section of giant fullerene cage C_{720} with over 800 encapsulated hydrogen atoms, approximately corresponding to 1% average relative C−C bond elongation at room temperature. Geometry is optimized using Tersoff−Brenner atomic potentials in combination with van der Waals potentials. Carbon and hydrogen atoms are shown in gray and white colors, respectively. Layer of thickness δ is unaccessible to hydrogen.

We also derive a general relation between the internal pressure and average relative C−C bond elongation in fullerene cages of various radii. Using the correspondence between the density and pressure of encapsulated hydrogen at either zero or finite temperature, we provide an estimate for the amount of hydrogen necessary to be confined at given strain in any fullerene nanocage. Our data demonstrate the excellent mechanical properties of the fullerene cages, which make them efficient nanocontainers with high theoretical capacity for hydrogen storage.

Acknowledgment. This work was supported by the Office of Naval Research (program manager Peter Schmidt) and partially by the DOE Hydrogen Sorption Center of Excellence, Contract DE-FC36-05GO15080. We are grateful to Kun Jiao for the semiempirical optimization of the $H_n@C_{720}$ giant endohedral fullerene, to Ming Hua and Yu Lin for their technical help, and to Vladimir I. Pupyshev, Betty C. Rostro, and Arta Sadrzadeh for stimulating discussions.

References

(1) Dresselhaus, M. S.; Dresselhaus, G.; Eklund, P. C. *Science of Fullerenes and Carbon Nanotubes*; Academic Press: San Diego, CA, 1996.
(2) Oku, T.; Narita, I.; Nishiwaki, A.; Koi, N.; Suganuma, K.; Hatakeyama, R.; Hirata, T.; Tokoro, H.; Fujii, S. In *Carbon, The Future Material For Advanced Technology Applications*; Messina, G., Santangelo, S.; Eds.;Springer-Verlag: Berlin, 2006. *Top. Appl. Phys.* **2006** *100* 187–216.
(3) Monthioux, M. *Carbon* **2002**, *40*, 1809–1823.
(4) Cioslowski, J. *J. Am. Chem. Soc.* **1991**, *113*, 4139–4141.
(5) Jones, D. E. H. *The Inventions of Daedalus*; Freeman: Oxford, 1982; *New Sci.* **1966**,–*32*, 245.

(6) Rubin, Y.; Jarrosson, T.; Wang, G.-W.; Bartberger, M. D.; Houk, K. N.; Schick, G.; Saunders, M.; Cross, R. J. *Angew. Chem., Int. Ed.* **2001**, *40*, 1543–1546.
(7) Komatsu, K.; Murata, M.; Murata, Y. *Science* **2005**, *307*, 238–240.
(8) Murata, Y.; Murata, M.; Komatsu, K. *J. Am. Chem. Soc.* **2003**, *125*, 7152–7153.
(9) Oksengorn, B. *C. R. Chimie* **2003**, *6*, 467–472.
(10) Avramov, P. V.; Yakobson, B. I. *J. Phys. Chem. A* **2007**, *111*, 1508–1514.
(11) Yakobson B. I.; Avramov, P. V.; Margrave, J. L.; Mickelson, E. T.; Hauge, R. H.; Boul, P. J.; Huffman, C. B.; Smalley, R. E. High-Yield Method of Endohedrally Encapsulating Species Inside Fluorinated Fullerene Nanocages: X@CF. U.S. Patent 7,252,812. B2, August 7, 2007.
(12) Züttel, A. *Naturwissenschaften* **2004**, *91*, 157–172.
(13) Ströbel, R.; Garche, J.; Moseley, P. T.; Jörissen, L.; Wolfd, G. *J. Power Sources* **2006**, *159*, 781–801.
(14) Ye, X.; Gu, X.; Gong, X. G.; Shing, T. K. M.; Liu, Z.-F. *Carbon* **2007**, *45*, 315–320.
(15) Barajas-Barraza, R. E.; Guirado-López, R. A. *Phys. Rev. B* **2002**, *66*, 155426.
(16) Türker, L.; Erkoç, *J. Mol. Struct.: THEOCHEM* **2003**, *638*, 37–40.
(17) Koi, N.; Oku, T. *Sci. Technol. Adv. Mater.* **2004**, *5*, 625–628.
(18) Koi, N.; Oku, T. *Solid State Commun.* **2004**, *131*, 121–124.
(19) Dolgonos, G. *J. Mol. Struct.: THEOCHEM* **2005**, *723*, 239–241.
(20) Dodziuk, H. *Chem. Phys. Lett.* **2005**, *410*, 39–41.
(21) Turker, L.; Erkoc, S. *Chem. Phys. Lett.* **2006**, *426*, 222–223.
(22) Dodziuk, H. *Chem. Phys. Lett.* **2006**, *426*, 224–225.
(23) Ren, Y. X.; Ng, T. Y.; Liew, K. M. *Carbon* **2006**, *44*, 397–406.
(24) Dodziuk, H. *J. Nanosci. Nanotechnol.* **2007**, *7*, 1102–1110.
(25) Ordejón, P.; Artacho, E.; Soler, J. M. *Phys. Rev. B* **1996**, *53*, 10441–10444.
(26) Soler, J. M.; Artacho, E.; Gale, J. D.; Garcfía, A.; Junquera, J.; Ordejón, P.; Sánchez-Portal, D. *J. Phys.: Condens. Matter* **2002**, *14*, 2745–2779.
(27) For further details of SIESTA software, see: http://www.uam.es/siesta/ website.
(28) Kohn, W.; Sham, L. J. *Phys. Rev.* **1965**, *140*, 1133–1138.
(29) Perdew, J. P.; Burke, K.; Ernzerhof, M. *Phys. Rev. Lett.* **1996**, *77*, 3865–3868. *Phys. Rev. Lett.* **1997**, *78*, 1396..
(30) Troullier, N.; Martins, J. L. *Phys. Rev. B* **1991**, *43*, 1993–2006.
(31) Sankey, O. F.; Niklewski, D. J. *Phys. Rev. B* **1989**, *40*, 3979–3995.
(32) *Gaussian Basis Sets for Molecular Calculations*; Huzinaga, S., Ed.; Elsevier: Amsterdam, 1984.
(33) Huber, K. P.; Herzberg, G. *Molecular Spectra and Molecular Structure. IV. Constants of Diatomic Molecules*; Van Nostrand: New York, 1979.
(34) Hedberg, K.; Hedberg, L.; Bethune, D. S.; Brown, C. A.; Dorn, H. C.; Johnson, R. D.; De Vries, M. *Science* **1991**, *254*, 410–412.
(35) For single encapsulated H_2 molecule, we calculate the formation energy $\Delta E = -0.5$ eV (cf. refs 4, 19, and 20). For comparison, H_2 physisorption on the hydrogen-terminated graphene patch $C_{32}H_{14}$, computed with the same method, yields $\Delta E = -0.2$ eV and the equilibrium distance from the hydrogen molecule center of mass to the graphene plane equal to 2.8 Å (H_2 situated over the center of hexagon, perpendicular to the plane). This somewhat overestimates the hydrogen binding to graphene, relative to the experimental data (see, e.g., Mattera, L.; Rosatelli, F.; Salvo, C.; Tommasini, F.; Valbusa, U.; Vidali, G.; *Surf. Sci.* **1980**, *93*, 515–525).
(36) Dumitrica, T.; Hua, M.; Yakobson, B. I. *Proc. Natl. Acad. Sci. U.S.A.* **2006**, *103*, 6105–6109.
(37) Herzberg, G. *Faraday Discuss.* **1981**, *71*, 165–173.
(38) Chen, Z.; Thiel, W.; Hirsch, A. *ChemPhysChem* **2003**, *4*, 93–97.
(39) Yakobson, B. I.; Avouris, P. In *Carbon Nanotubes*; Dresselhaus, M. S., Dresselhaus, G., Avouris, P., Eds.; Springer-Verlag: Berlin, 2001; *Top. Appl. Phys.* **2001**, *80*, 287−327.
(40) Hubbard, W. B.; Burrows, A.; Lunine, J. I. *Annu. Rev. Astron. Astrophys.* **2002**, *40*, 103–136.
(41) Itoh, S.; Ordejón, P.; Drabold, D. A.; Martin, R. M. *Phys. Rev. B* **1996**, *53*, 2132–2140.
(42) Matsuishi, K.; Gregoryanz, E.; Mao, H.-K.; Hemley, R. J. *J. Chem. Phys.* **2003**, *118*, 10683–10695.
(43) Huang, J. Y.; Ding, F.; Jiao, K.; Yakobson, B. I. *Phys. Rev. Lett.* **2007**, in press.

NL071436G